Journal of Physics: Conference Series

PAPER • **OPEN ACCESS**

Receiving antenna array element with extended bandwidth toward low frequencies

To cite this article: E V Balzovsky *et al* 2017 *J. Phys.: Conf. Ser.* **881** 012001

IOP Conf. Series: Journal of Physics: Conf. Series **881** (2017) 012001 doi:10.1088/1742-6596/881/1/012001

Receiving antenna array element with extended bandwidth toward low frequencies

E V Balzovsky, Yu I Buyanov, V I Koshelev and E S Nekrasov

Institute of High Current Electronics SB RAS, Tomsk, Russia

E-mail: koshelev@lhfe.hcei.tsc.ru

Abstract. An ultrawideband antenna based on a short dielectric dipole has been developed to sound dielectric layered media and to search objects including those hidden behind a dielectric barrier. In contrast to the previously presented antennas, the new one has an unbalanced output and contains a built-in balanced-to-unbalanced unit. As a result of optimization of the antenna geometry and topology of active elements, the lower frequency boundary was shifted toward low frequencies. The antenna records short nanosecond pulses with the spectrum ranging from 150 MHz to 2 GHz with small waveform distortions.

1. Introduction

Radar systems of short-range action based on sounding by short ultrawideband (UWB) pulses are used in geolocation, in the tasks of searching objects placed behind dielectric barriers or hidden inside of dielectric medium [1, 2]. The losses in the sounded medium increase with the frequency rise. To increase the depth of sounding, it is necessary to use UWB pulses of the length 1-4 ns. The spectrum of these pulses is shifted toward low frequencies and occupies the bandwidth of 0.15-2 GHz. The UWB transmitting antennas [3] have been developed for the effective excitation of electromagnetic pulses near the boundary with the dielectric medium.

To record reflected UWB electromagnetic pulses of the length 1-4 ns with small waveform distortions, receiving antennas are required. These antennas have the following properties: a) the voltage at the antenna output is proportional to the electric field strength; b) the antenna has small electrical dimensions; c) the phase center exists and it is constant; d) the antenna pattern retains the maximum position in the frequency range occupied by the pulse spectrum. These requirements correspond to active dipole antennas.

To reduce the frequency dependence of the dipole impedance, it is preferable to use a mismatched mode. The load of a short dipole is an active electronic circuit with the capacitive impedance [4]. The sensitivity of the antenna decreases due to the mismatch, but it is compensated by the insertion gain [5, 6]. Variants of the designs of such antennas for recording pulses of the length ranging from 0.5 ns to 2 ns are presented in [7, 8]. The lower frequency f_L of the operating bandwidth is limited by the value $f_L = 0.3$ GHz. To record pulses of the length 4 ns, it is necessary to shift f_L down to 0.15 GHz.

A specific feature of the above-mentioned active antennas is a balanced output. Its advantage is suppression of in-phase currents induced on the cable braid. However, the large dimensions and the complexity of the balanced-to-unbalanced network (balun) [7] make it difficult to use such an antenna as an element of the antenna array. To eliminate this disadvantage, it is proposed to use an integral-type balun mounted directly into the antenna. The design of a dipole antenna with a downward f_L, variants of its design with different types of baluns and the results of measurements of their characteristics are given below.

2. Design of antennas

Variants of the active antenna design that have the same electrical circuit of an active element but differ in the construction of a balancing circuit have been developed. The active element is balanced. Figure 1 presents the circuit of one channel of the active element. The arms of the dipoles are sectioned. To reduce the frequency dependence of the impedance, a resistor is installed into the break in the dipole arm [9]. A field-effect transistor ATF38143 Avago Technologies is included in the common-source scheme. At the supply voltage $V_c = 3$ V, the current consumption of each channel is no higher than 25 mA. The frequency properties of the four-terminal network are determined by the properties of the transistor itself and the nominal values of the circuit elements.

Figure 2a presents the circuit of the active antenna with an external balun (antenna AA1). The arms 1 and 2 of the dipole are connected to the input of the active circuit consisting of two identical amplifiers 3 and 4. The antenna is connected to the balun by two cables forming a shielded two-wire line 5. The external balun [7] consists of an inverter presenting two smooth transitions from a microstrip line to a two-wire line 6. These segments are included on opposite sides, with the strip of one line passing into the ground plate of the other line. A segment of the microstrip line 7 compensates the delay time of the signal τ_d in the inverter. The signals from the inverter and line 7 are summated in the summing unit 8. The selected antiphase signal component arrives to the output 9. The external balun is made on a separate printed circuit board of the size 160×45 mm.

Figure 1b presents the circuit of the antennas with the built-in balun. In this case, the antennas have an unbalanced output. The baluns are the available components with maximum bandwidth in the frequency range close to 0.1-2 GHz. Antenna AA2 contains a ceramic *Anaren* B0430J50100AHF balun made as a multilayer structure and has the dimension of 2×1.3×0.7 mm. Antenna AA3 contains a *Macom* ETC-1-13 transformer. It has a dimension of 4×3.8×2.8 mm and contains the symmetrical line made of a pair of wires twisted together. This line is wound on a ferrite core. Antenna AA4 contains a hand-made balancing transformer. The transformer is a two-wire line wound in 6 turns on a ferrite ring M2000NM of the dimension of 5×3×1.5 mm. The two-wire line is made in the form of two identical pieces of wire insulated in Teflon and twisted together.

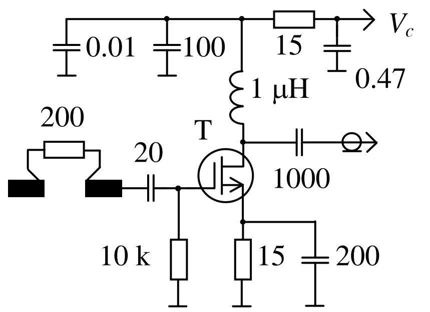

Figure 1. Principal diagram of the active antenna channel.

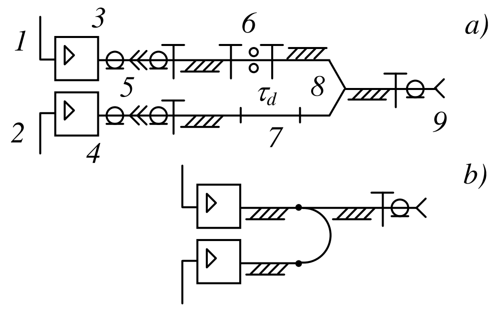

Figure 2. A diagram of the active antenna with the external (a) and built-in (b) baluns.

Figure 3 shows a physical configuration of the antennas. The antennas are printed on a fiberglass plate of the dimension 60×40×1 mm. Shoulders 1 and 2 of the dipole have a width of 8 mm. Elements 3 and 4 are transistors, element 5 is a balun. The outputs of the antennas present a semi-rigid coaxial cable. The supply voltage is fed by a separate wire 7.

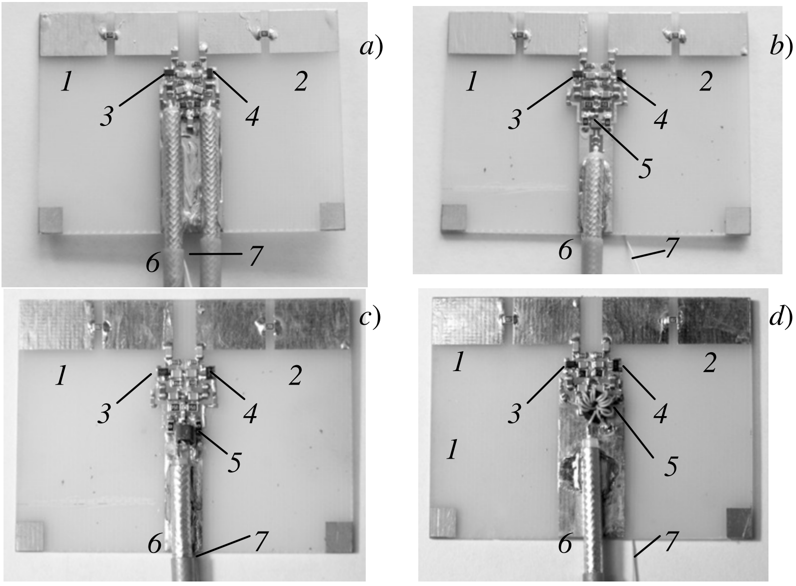

Figure 3. Physical configuration of the antennas: antenna AA1 (a) with a balanced output (the balun board is not shown); antennas AA2 (b), AA3 (c), and AA4 (d).

3. Characteristics of the antennas in the time domain

The measurements of the characteristics of the receiving antennas were made in the time domain. A set of four semiconductor generators of short UWB pulses and four combined antennas KA was used. Antenna KA1 was used at the excitation by bipolar voltage pulses of the length $\tau_p = 0.5$ ns by the level of 0.1 [10]. Antennas KA2 [11], KA3 [12], and KA4 [13] were used at the excitation by monopolar pulses with $\tau_p = 1$ ns, $\tau_p = 2$ ns, and $\tau_p = 3$ ns, respectively.

When measuring the shape of UWB pulses, a TEM-antenna with the ground plate size of 120×50 cm and the height of the antenna aperture of 8 cm was used as a reference receiving one [14]. The ratio of the peak voltage at the antenna output to the peak electric field strength at the receiving point is the effective height of the antenna h_e. For a TEM-antenna, h_e does not depend on the frequency in a wide range and is equal to half the height of the aperture [14]. For the above-indicated TEM-antenna, $h_e^{TEM} = 4$ cm.

Figure 4 presents the temporal waveforms of voltage pulses $V_{AA}(t)$ at the outputs of receiving antennas AA1-AA4 and voltage pulses $V_{TEM}(t)$ at the output of the TEM-antenna.

To quantify the distortions of the temporal waveform of the pulses, the root-mean-square (RMS) deviation σ of the voltage waveform $V_{AA}(t)$ at the output of the studied antennas AA1-AA4 and the voltage $V_{TEM}(t)$ was calculated according to the ratio:

$$\sigma = \left(\frac{\int_T \left[v(t - t_0) - u(t) \right]^2 dt}{\int_T u^2(t)\, dt} \right)^{1/2},$$

where $u(t) = V_{TEM}(t)\left(\int_T V_{TEM}^2(t')\, dt'\right)^{-1/2}$ and $v(t) = V_{AA}(t)\left(\int_T V_{AA}^2(t')\, dt'\right)^{-1/2}$ are the normalized functions, T is the time window, and the value t_0 is found as a result of an iterative procedure for minimizing the σ value. Table 1 presents the results of calculation of σ at for various values of τ_p. Significant distortions in the waveform of the pulses of antenna AA2 can be caused by the too narrow bandwidth of the used integral balun. Table 2 presents the values of h_e^{AA} for various τ_p.

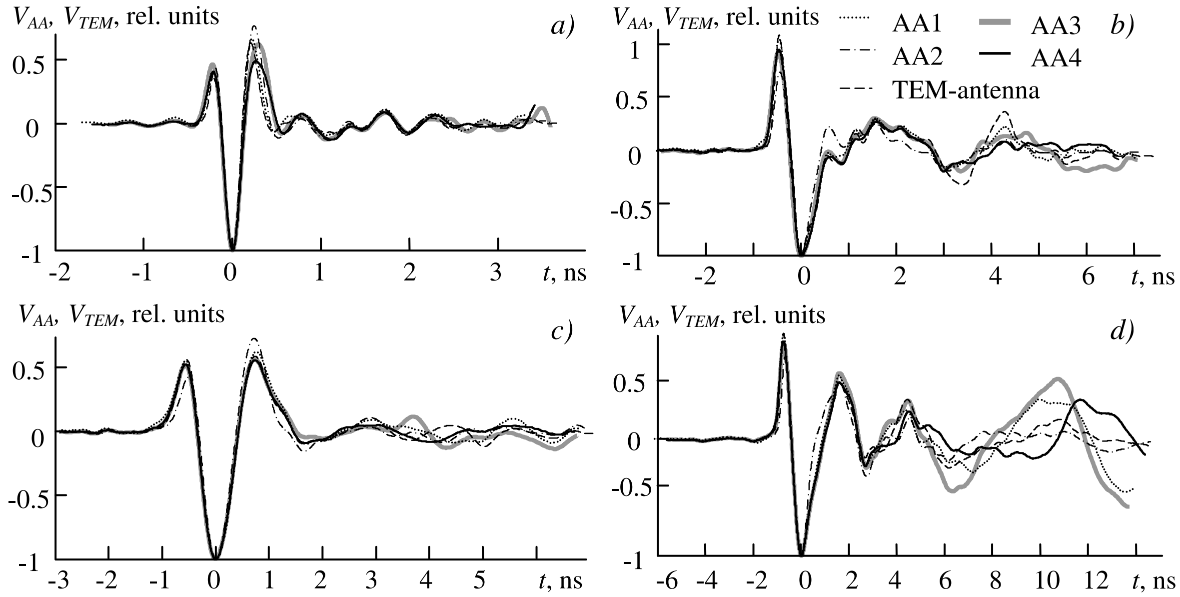

Figure 4. Waveforms of the pulses at the outputs of receiving antennas AA1-AA4 in cases when KA 1 is excited by bipolar pulses of the length 0.5 ns (a); KA 2 is excited by monopolar pulses of the length 1 ns (b); KA 3 is excited by bipolar pulses of the length 2 ns (c); and KA 4 is excited by bipolar pulses of the length 3 ns (d).

Table 1. RMS deviation of receiving antennas σ versus the pulse length of the generator.

Receiving antenna	τ_p = 0.5 ns	τ_p = 1 ns	τ_p = 2 ns	τ_p = 3ns
A1	0.12	0.12	0.08	0.08
A2	0.28	0.35	0.22	0.33
A3	0.4	0.15	0.06	0.1
A4	0.4	0.16	0.1	0.14

Table 2. Effective height h_e^{AA} of receiving antennas (in cm) versus the pulse length of the generator.

Receiving antenna	τ_p = 0.5 ns	τ_p = 1 ns	τ_p = 2 ns	τ_p = 3 ns
A1	0.6	0.78	0.86	0.8
A2	0.37	0.5	0.47	0.5
A3	0.27	0.4	0.45	0.45
A4	0.3	0.4	0.45	0.44

4. Antenna characteristics in the frequency domain

To find the frequency dependence of the effective height of the active antenna $h_e^{AA}(f)$ from the measured values of $V_{AA}(t)$, the spectrum $S_{AA}(f)$ was calculated using the Fourier transform, and the spectrum $S_{TEM}(f)$ was calculated from the measured values of $V_{TEM}(t)$. The desired quantity is determined by the following expression:

$$h_e^{AA}(f) = h_{TEM}^{e} \frac{S_{AA}(f)}{S_{TEM}(f)}.$$

Since the frequency bandwidth of the receiving active antenna is wider than the spectrum of radiation of a single KA, the measurements of $h_e^{AA}(f)$ were carried out using a set of antennas and pulse generators with different values of τ_p. Figure 5 shows the frequency dependence of the $h_e^{AA}(f)$ module. Figure 6 shows the deviation of the $h_e^{AA}(f)$ phase ($\Delta\varphi$) from the linear dependence. Curves 1 in the Figures 5 and 6 correspond to the spectrum of the pulses radiated by antenna KA 4 excited by bipolar pulses with $\tau_p = 3$ ns. Curves 2 correspond to the spectrum of the pulses radiated by antenna KA 3 excited by bipolar pulses with $\tau_p = 2$ ns. Curve 3 corresponds to the spectrum of the pulses radiated by the antenna KA 2 excited by monopolar pulses with $\tau_p = 1$ ns. Curve 4 corresponds to the spectrum of the pulses radiated by the antenna KA 1 excited by bipolar pulses with $\tau_p = 0.5$ ns. For antenna AA1 with the external balun, the bandwidth of operating frequencies, determined as the smallest frequency band in which $\left|h_e^{AA}(f)\right|$ changes by no more than 3 dB and $\Delta\varphi$ changes in the limits of ±11.25, equals to 0.12-2.5 GHz. For the antenna AA2 with the built-in balun, the frequency bandwidth in which the amplitude of the relative effective length varies within 3 dB equals to 0.3-2.2 GHz. However, a phase shift in the entire range results in significant distortion of the waveform of the recorded pulses. The bandwidth for antennas AA3 and AA4 is 0.15-2 GHz and 0.1-2 GHz, respectively.

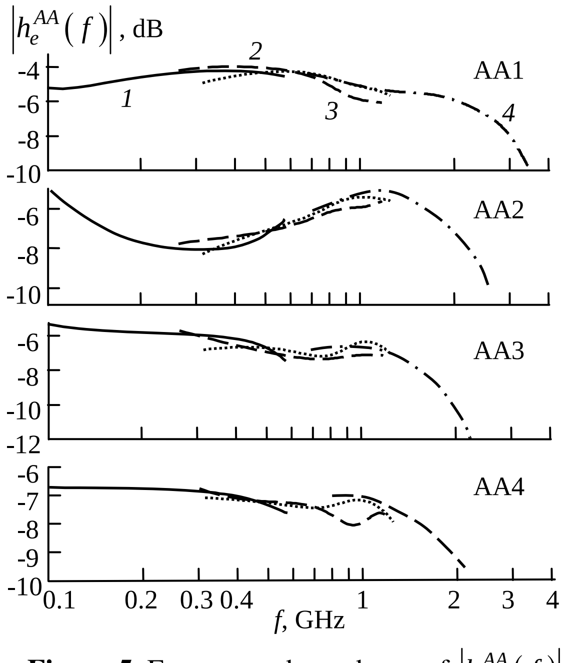

Figure 5. Frequency dependence of $\left|h_e^{AA}(f)\right|$.

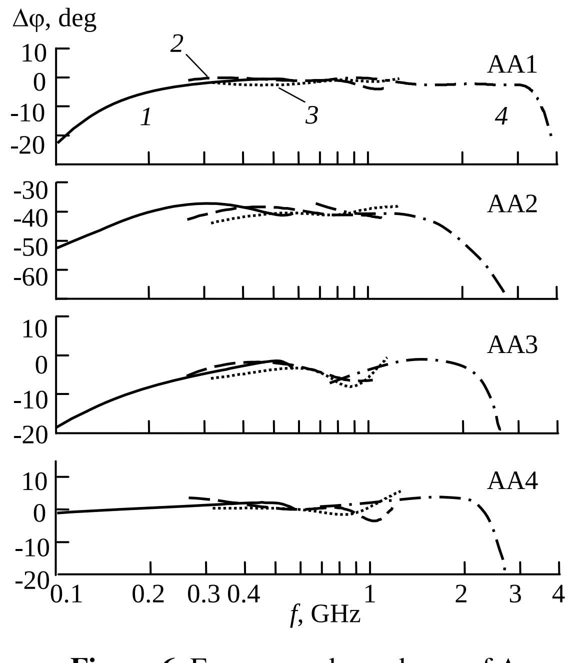

Figure 6. Frequency dependence of $\Delta\varphi$.

5.Conclusion

The developed and researched variants of the active dipole receiving antenna with the built-in balun on the basis of ferrite transformers allow recording electromagnetic pulses of the length 1-4 ns with small distortions. The spectrum of the pulses occupies the frequency bandwidth of 0.15-2 GHz. Further research will be aimed at creating an antenna array based on the developed antennas.

Acknowledgment
The work was supported by the Russian Science Foundation, the project #16-19-10081.

IOP Conf. Series: Journal of Physics: Conf. Series **881** (2017) 012001 doi:10.1088/1742-6596/881/1/012001

References

[1] Daniels D J 2004 *Ground-penetrating radar – 2nd ed.* (London: The Institution of electrical engineers) p 734
[2] Sachs J 2012 *Handbook of ultra-wideband short-range sensing* (Weinheim, Germany: Wiley–Interscience) p 824
[3] Zwick T 2013 *Ultra-wideband RF system engineering* (UK: Cambridge University Press) p 186
[4] Copeland J R, Robertson W J and Verstraete R G 1964 *IEEE Trans. Antennas Propag.* **12** 227
[5] Yoon I J, Balzovsky E, Buyanov Yu, Park S H, Kim Y and Koshelev V 2007 *Microwave Opt. Technol. Lett.* **49** 2998
[6] Balzovskii E V, Buyanov Yu I and Koshelev V I 2007 *Rus. Phys. J.* **50** 503
[7] Balzovskii E V, Buyanov Yu I and Koshelev V I 2010 *J. Commun. Technol. Electron.* **55** 172
[8] Balzovsky E V, Buyanov Y I, Koshelev V I and Nekrasov E S 2016 *Rev. Sci. Instr.* **87** 034703
[9] Einzlger P D, Leviatan Y and Rozenkovich J 1989 *Microwave Opt. Technol. Lett.* **2** 208
[10] Efremov A M, Koshelev V I, Kovalchuk B M, Plisko V V and Sukhushin K N 2011 *Instrum. Exper. Techn.* **54** 70
[11] Andreev Yu A, Buyanov Yu I and Koshelev V I 2005 *J. Commun. Technol. Electron.* **50** 535
[12] Koshelev V I, Andreev Yu A, Efremov A M, Kovalchuk B M, Plisko V V, Sukhushin K N and Liu S 2012 *J. Energy Power Eng.* **5** 771
[13] Gubanov V P, Efremov A M, Koshelev V I, Kovalchuk B M, Korovin S D, Plisko V V, Stepchenko A S and Sukhushin K N 2005 *Instrum. Exper. Techn.* **48** 312
[14] Koshelev V I, Buyanov Yu I and Belichenko V P 2017 *Ultrawideband short-pulse radio systems* (Artech House) p 432